

Design and performance of prototype muon detector of LHAASO-KM2A

G. XIAO¹, X. ZUO¹, X.R. LI¹, S.H. FENG¹ FOR THE LHAASO COLLABORATION.

¹ Key Laboratory of Particle Astrophysics, Institute of High Energy Physics, CAS, Beijing 100049, China

xiaog@ihep.ac.cn

Abstract: LHAASO envisages constructing a large area of muon detector array which includes 1221 muon detectors at the elevation of 4300 m. The array will be used to discriminate gamma showers from hadronic ones by measuring the muon components of the showers. A muon detector prototype has been built in Tibet and the performance of the detector is studied. In this paper we present the design features, the technical characteristics and the data performance of the prototype. Moreover, the punch-through effect of shower electromagnetic components, the long-time stability and the position dependence of signals will also be discussed.

Keywords: Muon detector prototype, Water-Cherenkov detector

1 Introduction

As the main array of the large high altitude air shower observatory (LHAASO)[1], the one Kilometer square extensive air showers array (KM2A) has two major targets, i.e. searching for sources of ultrahigh energy cosmic rays and study of cosmic ray physics in an energy range from 20TeV to 100PeV. KM2A is expected to reach a sensitivity of 1% Crab flux unit for γ -ray point sources at 50TeV, which requires detecting at least 10 γ rays from a single source each year. To measure such a low flux, we need a detector array with an effective area of one square kilometer working with full duty cycle and performing background-free detection of gamma rays at this energy. Only ground-based air shower arrays can fulfill such requirements. Since the flux of background cosmic rays is 4-5 orders higher than gamma rays, the γ /hadron discrimination must be taken into consideration and a rejection power of 10^4 is needed. The measurement of muons could achieve the most effective γ /hadron discrimination because hadron induced showers contain much more muons than gamma-ray ones.

Through detailed Monte Carlo simulations[2][3] different designs of the KM2A array are studied. The final design for LHAASO-KM2A is one square kilometer with 5635 electromagnetic particle detectors (EDs) and 1221 muon detectors (MDs). Each ED is designed to be 1 square meter of scintillator with 15 meters spacing. Each MD is designed to be a water Cherenkov tank of 36 square meters with 30 meters spacing. The optimization of the sizes and distances of the detectors is carried out by simulating the array with different sizes and distances of EDs and MDs and comparing the simulated sensitivities of the array. The sensitivity of the final designed array is high enough for fulfilling the main targets.

For LHAASO-KM2A, 1221 muon detectors with 3.4m in radius and 1.2m in height will be constructed in Yunnan province of China. Each muon detector includes a 6.8m-diameter concrete tank containing a sealed liner with a reflective inner surface. The liner contains 44t of purified water. Cherenkov light produced by the passage of particles through the water is collected by one eight-inch-diameter PMT which resides at the top center of the liner and looks downwards through a special optical window. In order to shield against the electromagnetic compositions of air showers, 2.5 m of dirt above the muon detector will be

used as absorbing layer. The general components of a muon detector are shown in Fig. 1.

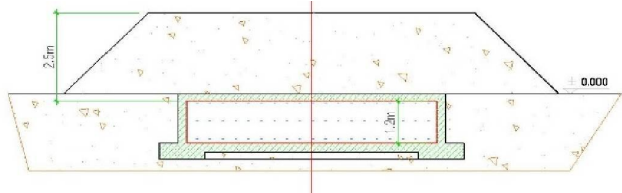


Fig. 1: schematic view of a MD

On January, 2013, a water-Cherenkov muon detector prototype was installed at Yangbajing, Tibet and has been operated stably. Fig. 2 is the overview of the tank prototype before covered by dirt as the shield. Performances of the detector prototype will be presented in this paper, which include the single peak of muon, position dependence, punch-through effect and long-term stability. The design features and the detector optimization are also presented.



Fig. 2: Overview of the MD prototype at Yangbajing before covered by dirt

2 Design and optimization

2.1 Geometry

The area of a MD unit is defined by simulation of the whole array, while its height is optimized by simulation with Geant4. The Geant4-based simulation code produces Cherenkov photons along the path of the injected muons and tracks them through the water until they are absorbed or they reach the active area of the PMT photocathode. Figure. 3 shows the number of photoelectrons on the PMT varying with water depth and absorption length (the liner reflectivity is set to 97.5%). Under the same water depth, Npe increases with absorption length. As the water depth increases, Npe initially increases due to longer muon track length and then decreases when water absorption exceeds the increase of track length.

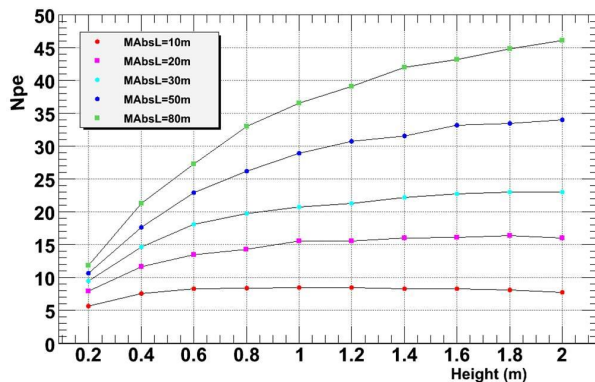


Fig. 3: The number of photoelectrons from the simulation varying with height of the tank water

According to experiences of other experiments using the same technique, a water absorption length $> 30m$ is easy to be achieved. The height of MD water tank is chosen as 1.2m since Npe is required to be > 20 . With such detector geometry and overburden dirt of 2.5m, simulation shows that Npe by shower secondary γ is negligible with a detection efficiency of about seven per million.

2.2 Liner

Tank liners are right circular cylinders made of flexible plastic material which can conform to the inside surface of the concrete tanks. The liner has a diameter of 6.8 m and a height of 1.2 m and fulfills three functions. First, it can enclose the water volume, prevent chemical contamination and active microbe, and provide a barrier against any external light to enter the water tank volume; Second, it is used to diffusively reflect Cherenkov light produced by muons that traverse the water[4]; And third, it provides optical access for the PMTs to collect the Cherenkov lights.

In the design process of the liner, five characteristics are taken into consideration[4], which are the strength, strong diffuse reflectivity of its inner surface for Cherenkov light, good sealability, excellent chemical resistance, and prevention against contamination of microbe and precipitate.

The liner is made of separate laminates by proper processing method, each laminate is composed of three layers of co-extruded materials (see Fig. 4). The inner is made of Tyvek 1082D (DuPont), which is an opaque material with excellent strength, good flexibility and big diffuse reflectivity for near ultraviolet lights. The Tyvek is non-woven material made of high density polyethylene, which can minimize

the possibility of chemicals leaching into the water volume. The middle layer is made of LDPE film with good strength and outstanding chemical resistance. PP film is chosen as the outer layer because of its hard-wearing.

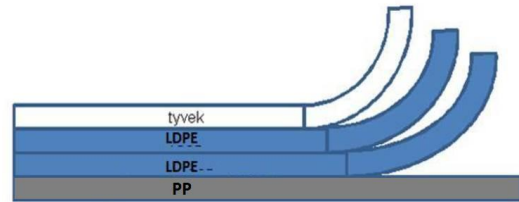


Fig. 4: Cross section of the liner.

Liner is assembled by firstly processing two laminates from inside to outside of the three-layer of material, and then welding them together. Two of the laminates are the top and bottom respectively. The liner will shape into a cylinder voluntarily when it is filled with water in a columnar tank. On the top of the liner, there are one window and two fill ports with screw caps hermetically sealed to them. The window is a transmission cover made of EVA, a kind of optical plastic. The fill ports are used to inject water to the liner and discharge water when needed. Fig. 5 shows the liner filled with air.



Fig. 5: The liner filled with air.

2.3 PMT enclosure and assembly

The PMT enclosure system is showed in Fig. 6. This allows the PMT to collect Cherenkov lights from the water volume. This equipment can protect the PMT and also provides a cover to shield the PMT from external lights.

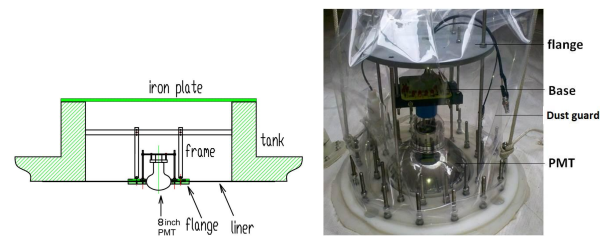


Fig. 6: The section view of the assembling of EVA cover and PP plate flange with inlet, outlet ports in it and nuts sealed in it.

The window is made of EVA plastic, which is formed according to the shape of PMT photocathode and heat-

sealed to a hole in the top laminate of the liner. Above the EVA window, there is an annular PP plate flange adhered to the liner, with nuts sealed in it.(see Fig. 6). The flange is used to support the liner top and maintain the liners normal cylindrical shape when the liner is installed into the concrete tank and filled with purified water. The space between the window and the PMT photocathode is filled with silicone oil[4] for optical coupling. The PMT could be protected by these enclosures from external lights and possible damage caused by surrounding medium.

3 Performance of the prototype

A MD prototype as installed in the concrete tank (Fig. 2) at Yangbajing on January, 2013. The PMT used for the prototype is HAMAMATSU R5912 with positive high-voltage supply. Five movable scintillators (four on the top and 1 in a tunnel below the tank) are used to select incident muons with different positions and directions. The data acquisition system used is the VME-9U chassis with FEE plug-in module which mainly record the time and charge of signals exceeding a configurable threshold. The whole waveform of the muon signals at different injecting positions were also recorded by a digital oscilloscope. The detector performance of single muon spectrum, position dependence, punch through effect and long time stability have been studied.

3.1 Single muon waveform

When a high energy muon passes through the water tank, it produces hundreds of Cherenkov photons per centimeter. The Cherenkov lights propagate in the water and can be reflected by the inner Tyvek of the liner. At last some of the photons can arrive at the PMT on the top and generates electronic signals. The FEE data taking system can record the time and charge of signals, and an oscilloscope was used to record the whole waveform. Fig. 7 is the an example single muon waveform. The signal lasts for hundreds of nanoseconds, confirming both the water quality and liner reflectivity are very high.

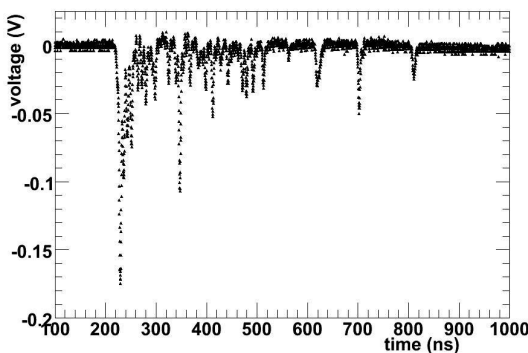


Fig. 7: An example single muon waveform.

3.2 Position dependence

Cherenkov photons generated by muons with with different injection positions travel different paths and suffer different attenuation by the water and liner, thus MD signal somehow depends on the position of the incident muons. Five movable scintillators (four on the top and 1 at the bottom) are used to select the incident muons with different positions and

directions. Npe of vertical muons hitting at 0m to 3m from the tank center is shown in Fig. 8, from which one can see Npe decreases when the muon track gets farther from the detector center. For vertical muons uniformly distributed in the tank area, an average Npe of about 35 is expected and a variation of less than 15% due to muon injection positions.

Fig. 9 shows Npe from vertical and slant muon events with different injection positions. The left four dots correspond to vertical muons mention above, while the right 4 are measured by putting the bottom scintillator at 2m and top scintillator at -1m 0m, 1m, 3m respectively. For slant events, Npe is corrected by its zenith angle in tank water, which can also be done when analyzing shower events.

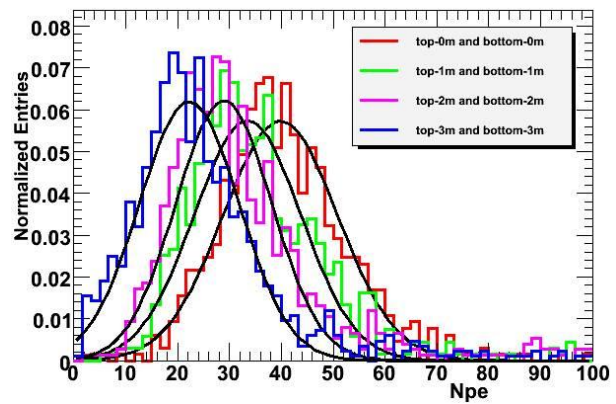


Fig. 8: Npe for vertical muon events with different injection positions

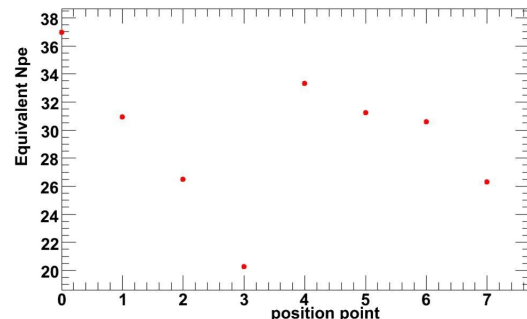


Fig. 9: The charge of signal generated by muon with different injection positions

3.3 Punch-through effect

The MD should eliminate the electromagnetic components of shower secondary particles, which ensures high purity of muons detected by MD. Since the energies of most electromagnetic particles in showers are much lower than muons, a certain thickness of soil layer could almost completely deposit them while muons can easily pass through and enters the tank water. A layer of 2.5m dirt corresponds to about 12 radiation length which is comparable to the air depth between 4300m altitude and sea level. At sea level, muons dominant secondary cosmic rays, while at an altitude of 4300m, shower gammas and e^\pm dominant.

Table 1 shows the trigger rate (triggered by the top and bottom scintillators) varying with different height of dirt on the prototype. As expected, it decreases with thicker

overburden dirt. This is due to both geometry and absorption of electromagnetic particles. The corrected trigger rate after considering the geometry are also listed in Table 1, from which one can see that the corrected trigger rate decreases at the beginning and then goes flat, hinting only muons pass through the tank at the end.

Thickness of the dirt (m)	0	0.7	1.75	2.3
Trigger rate/Hz	1.33	0.844	0.428	0.324
Corrected trigger rate/Hz/m ²	218.8	173.2	161.0	159.3

Table 1: The trigger rate varying with thickness of overburden dirt on the prototype.

Even most of the electromagnetic particles are absorbed by the overburden dirt, there exist some high energy gammas/ e^\pm punching-through the dirt and entering the tank water, thus contaminating the muons signals. The water tank (compared with scintillation detectors) can discriminate muon signals from electromagnetic ones according to the detected Npe due to that the total energy deposited by muons are, in average, much larger than that by punching-through electromagnetic particles.

3.4 Long-term stability

The muon detector has been operating in Tibet for more than five months, its long-term stability is studied via data analyses. The prototype is triggered by coincident events of the top and bottom scintillation detectors vertically aligned with a distance of 2m to the tank center. A stable trigger rate between 0.3 Hz 0.32 Hz is observed. The prototype detection efficiency is higher than 97% and is very stable. Fig. 10 shows number of photoelectrons (Npe) varying with time. In this figure, Npe is normalized to that in the first day. Npe is very stable in 5 months.

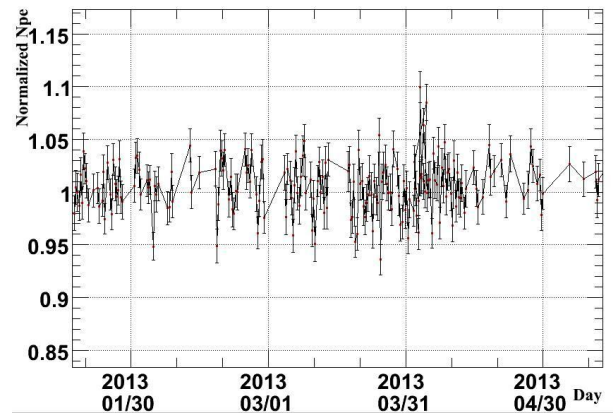


Fig. 10: The normalized number of photon electrons

Icing of the tank water will introduce damage to the liner surface, the PMT window and even the PMT. At an altitude of 4,300 m, the annual maximum variation of environmental temperature can be as large as $\pm 30^\circ\text{C}$ (see Fig. 11). During winter, the daily average of environmental temperature is about -15°C . It is somewhat a big challenge to keep the tank water from freezing under such an environment. Fortunately, the overburden dirt acts not only as shield to shower electromagnetic components, but also as heat insulator. From Fig. 11 one can see that the environmental

temperature reaches the lowest in the end of January, while the temperature of the tank water reaches the lowest in the end of February, with a time delay of more than one month. This is consistent with estimation from thermal capacity of tank water and thermal conductivity of the overburden dirt. The lowest temperature of the tank water is about 0.3°C . It should be noted that the water temperature was below 2°C before the tank was fully covered by dirt in January which was the coldest period in one year. The water temperature is expected to be higher in the coming January, thus is the lowest temperature of the water in the coming year. The candidate LHAASO site has the same altitude as Yangbajing and the environmental temperature and the maximum seasonal frozen depth there are more or less the same, we expect that the MDs can pass safely the coldest seasons without freezing.

It's worthy to be mentioned that the overburden dirt reduces the temperature variation of the tank water, thus provides a stable environment to the PMT.

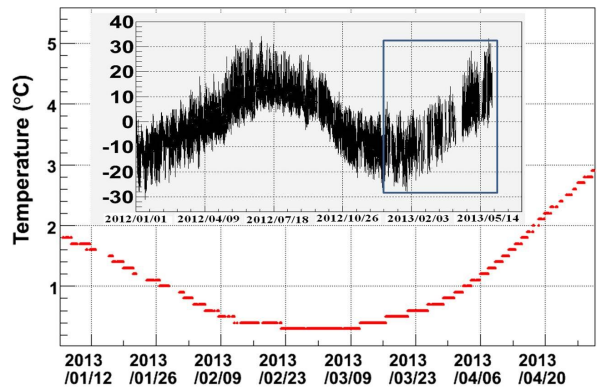


Fig. 11: The temperature outside (red) and inside (inner panel) the prototype, the square in the inner panel shows the period after the prototype was fully covered by dirt.

4 Summary and Conclusions

A muon detector prototype for LHAASO-KM2A was designed and constructed at YBJ cosmic ray observatory and has been in stable operation for more than 5 months. Its performances fully meet the design. Through the monitoring of the number of photoelectrons produced by single muon we conclude that both the water quality and the whole prototype are very stable. The detector can safely pass the coldest seasons without freezing at an altitude as high as 4300m.

References

- [1] Z. Cao et al, LHAASO Collaboration, in: Proceedings of 31st ICRC, 2009.
- [2] X.H. Ma et al., LHAASO Collaboration, in: Proceedings of 31st ICRC, 2009.
- [3] S.W. Cui et al., LHAASO Collaboration, in: Proceedings of 32st ICRC, 2011.
- [4] I. Allekotte et al., Nuclear Instruments and Methods in Physics Research A 586 (2008) 409C420
- [5] A. Etchegoyen et al., Nuclear Instruments and Methods in Physics Research A 545 (2005) 602C612